ELSEVIER

Voltage-gated sodium channels: structures, functions, and molecular modeling

Lei Xu[1,‡], Xiaoqin Ding[2,‡], Tianhu Wang[1,‡], Shanzhi Mou[3], Huiyong Sun[4] and Tingjun Hou[5]

[1] Institute of Bioinformatics and Medical Engineering, School of Electrical and Information Engineering, Jiangsu University of Technology, Changzhou 213001, China
[2] Beijing Institute of Pharmaceutical Chemistry, Beijing 102205, China
[3] School of Mathematics and Physics, Jiangsu University of Technology, Changzhou 213001, China
[4] Department of Medicinal Chemistry, School of Pharmacy, State Key Laboratory of Natural Medicines, China Pharmaceutical University, Nanjing 210009, China
[5] College of Pharmaceutical Sciences, Zhejiang University, Hangzhou 310058, China

Voltage-gated sodium channels (VGSCs), formed by 24 transmembrane segments arranged into four domains, have a key role in the initiation and propagation of electrical signaling in excitable cells. VGSCs are involved in a variety of diseases, including epilepsy, cardiac arrhythmias, and neuropathic pain, and therefore have been regarded as appealing therapeutic targets for the development of anticonvulsant, antiarrhythmic, and local anesthetic drugs. In this review, we discuss recent advances in understanding the structures and biological functions of VGSCs. In addition, we systematically summarize eight pharmacologically distinct ligand-binding sites in VGSCs and representative isoform-selective VGSC modulators in clinical trials. Finally, we review studies on molecular modeling and computer-aided drug design (CADD) for VGSCs to help understanding of biological processes involving VGSCs.

Introduction

VGSCs (or Na_vs) are heteromeric transmembrane proteins that are activated in response to membrane depolarization and have a fundamental role in the generation and propagation of action potentials in neurons and other electrically excitable cells via control of the flow of Na^+ ions through cell membranes. VGSCs belong to the voltage-gated ion channel (VGIC) superfamily, and each eukaryotic VGSC comprises a single polypeptide chain of α-subunit (~2000 residues) that folds into four homologous but nonidentical domains (DI to DIV) and one or more auxiliary β-subunits [1]. VGSCs are closely associated with a spectrum of physiological processes [2]. More than 1000 disease-related mutations of nine VGSC-encoding genes implicated in channel dysfunctions and channelopathies have been identified so far [3,4], and VGSCs have been regarded as appealing druggable targets for epilepsy, cardiac arrhythmias, and neuropathic pain [5]. For a long time, the design of isoform-selective VGSC modulators was challenging owing to the lack of co-crystallized protein–ligand structures and high sequence conservation in the channel pores across VGSC isoforms. However, X-ray [6–11] and cryo-electron microscopy (cryo-EM) structures [12–17] of VGSCs have been gradually resolved. In 2011, Payandeh *et al*. determined the first X-ray crystal structure of the bacterial *Arcobacter butzleri* VGSC (Na_vAb) [6]. In 2017, Shen *et al*. reported the first near-atomic resolution structure of a eukaryotic VGSC (Na_vPaS) from American cockroach by cryo-EM [12]. In 2018, Pan *et al*. identified the cryo-EM structure of the human $Na_v1.4$-β1 complex [14]. In 2019, Shen *et al*. reported the cryo-EM structure of human $Na_v1.7$ in complex with auxiliary subunits and animal toxins [17]. These structures provide a solid foundation for structure–function studies and rational structure-based design of new therapeutics.

In this review, we summarize the structures and functions, major ligand-binding sites, and representative isoform-selective

Corresponding authors: Sun, H. (huiyongsun@cpu.edu.cn), Hou, T. (tingjunhou@zju.edu.cn)
‡ These authors contributed equally.

https://doi.org/10.1016/j.drudis.2019.05.014

modulators of VGSCs. We also emphasize advances on molecular modeling and CADD of VGSCs.

The structures and functions of VGSCs

VGSCs occur across the prokaryotic and eukaryotic kingdoms. The α-subunit of VGSCs forms the core of the channel that conducts the flow of Na^+ ions in a voltage-gated manner. Each α-subunit of eukaryotic VGSCs has four domains (DI-DIV) linked by large intracellular loops and each domain contains six α-helical transmembrane segments (S1-S6) (Fig. 1a,b). In mammals, there are ten different isoforms of α-subunits, $Na_v1.1$–$Na_v1.9$; Na_x. $Na_v1.1$, $Na_v1.2$, $Na_v1.3$, and $Na_v1.6$ are predominantly expressed in the central nervous system (CNS), whereas $Na_v1.4$ is mainly expressed in skeletal muscle. $Na_v1.5$ is primarily expressed in cardiac muscle, and $Na_v1.7$, $Na_v1.8$ and $Na_v1.9$ are generally abundant in the peripheral nervous system. The sequence homology of the mammalian α-subunits is >70%, which makes it difficult to design isoform-selective modulators towards a specific VGSC [18]. To date, five β-subunits have been identified in vertebrates (β1, β1B, β2, β3, and β4), which have a prominent role in modulating the expression and membrane trafficking of the α-subunit, channel activation and inactivation, and ligand binding. Each β-subunit comprises an N-terminal extracellular immunoglobulin (Ig) domain, a single transmembrane (TM) α helix, and a small intracellular C-terminal region. The recently published cryo-EM structure of $Na_v1.4$ from electric eel ($EeNa_v1.4$) in complex with the β1-subunit presents a first glimpse into the interactions between the α- and β-subunits [13]. The S1–S4 segments form the voltage-sensing domain (VSD), characterized by a voltage sensing-responsible 'gating charges' cluster with four to eight, repetitively occurring, positively charged Arg/Lys residues within each S4 [19]. Each VSD is connected to the pore domain (PD) by an intracellular S4–S5 linker, and has different sequence signatures, conformations, and even roles in channel-gating modulatory effects [12]. For instance, the sequence lengths of the S2–S4 segments in the four domains of $hNa_v1.4$ are different, and the numbers of the gating charged residues in the four S4 segments vary from four to six (i.e., RRRK in DI, RRRKK in DII, KRRRRR in DIII, and RRRRRR in DIV), providing the molecular basis for the asynchronous movements of the VSDs in voltage-dependent activation [14].

PD comprises the S5–S6 segments and the extracellular linkers (P-loop), which enclose the central aqueous pore of the channel; each P-loop is separated into two α helices (P1 and P2) [12]. The asymmetric SF of human VGSCs is formed by the side chains of the signature DEKA motif (Asp/Glu/Lys/Ala) in the P-loop of each domain and a wide inner site formed by the carbonyl oxygens of the two preceding residues in each domain, including Thr/Gln (DI), Cys/Gly (DII), Thr/Phe (DIII), and The/Ser (DIV) [14]. There is an outer electronegative ring on the first helical turn of the P2 pore helix above the SF, Glu/Glu/Asp/Asp (EEDD), which has an important role in Na^+ permeation and the binding of tetrodotoxin (TTX). Analysis of the cryo-EM structure of Na_vPaS in complex with toxins suggests that the carboxylate group of an invariant Glu on P2 in DII and the DE residues in the DEKA motif constitute a highly electronegative site (DEE site) and a Na^+ ion is coordinated by this site [15]. The SF forms the narrowest constriction site along the permeation path in the pore domain and determines Na^+ selectivity.

Recent studies of bacterial VGSCs demonstrated that there are additionally lateral lipid-filling openings in the walls of the cytoplasmic pore, named fenestration, which connect the hydrophobic membrane to the central cavity [6]. Fenestrations may provide access to small hydrophobic VGSC blockers from the hydrophobic membrane to cytoplasmic binding site. A tethered cytoplasmic inactivation gate in mammalian VGSCs comprises a short intracellular loop between DIII and DIV, and confers fast inactivation through a potential allosteric blocking mechanism. The inactivation gate has an α-helix backbone, with the well-conserved hydrophobic Ile-Phe-Met (IFM) triplet located in this motif. The intracellular activation gate was originally presumed to be at the inner end of the pore. In response to membrane depolarization, the activation gate opens. The cryo-EM structures of $EeNa_v1.4$ confirmed that this activation gate is positioned at the cytoplasmic boundary level of the membrane [13].

The typical open–closed–inactivated cycle

There are at least three primary states for a typical VGSC (Fig. 1c): resting (closed), activated (open), and inactivated (closed). Upon membrane depolarization, the voltage sensors in the S4 helices move toward the extracellular surface, which stimulates the channel gate to open briefly (<1 ms). Then, Na^+ ions move into the cell, subsequently depolarizing the membrane, which is responsible for the rising phase of an action potential. After a few milliseconds, the sodium channels are rapidly inactivated, which is partially responsible for the falling phase of an action potential and results in its termination. Fast inactivation occurs over a timescale of ~1–5 ms and the channel stops ion conduction while the voltage sensor is still in an active conformation, mediated by the well-conserved IFM triplet located in the intracellular loop of DIII and DIV. The channel then enters a slow inactivated state in response to prolonged depolarization or rapid repetitive stimulations, which occur on the timescale of seconds to minutes. However, the structural basis for slow inactivation has not yet been elucidated. When the gating charged residues of each S4 return to their resting positions upon membrane repolarization, the sodium channel recovers from inactivation and deactivates (i.e., the activation gate closes). Therefore, the outward and inward movements of S4 lead to the opening and closing states of the pore domain.

Toxin and drug receptor sites of VGSCs

VGSCs are the targets of a variety of natural neurotoxins. Natural toxins and synthesized molecular modulators of VGSCs can be roughly categorized into two classes: pore blockers and gating modifiers. Pore blockers physically block the pore and inhibit channel conductance by binding to the extracellular loops and/or the pore. Gating modifiers stabilize the channel in a particular functional state and alter the generation and propagation of action potentials, which include toxins binding to intramembrane or extracellular receptor sites [17,20]. To date, eight binding sites of VGSCs for toxins and small molecules have been identified (Fig. 2 and Table 1); in-depth analysis of these binding sites at the molecular level provides valuable information to understand the structure–function relationships of VGSCs and to develop novel isoform-selective agents to treat VGSCs-related diseases [5].

Site 1: extracellular pore blocker

Binding site 1 is formed by the four P-loops and is located in proximity to the ion selectivity filter. This site can be occupied by

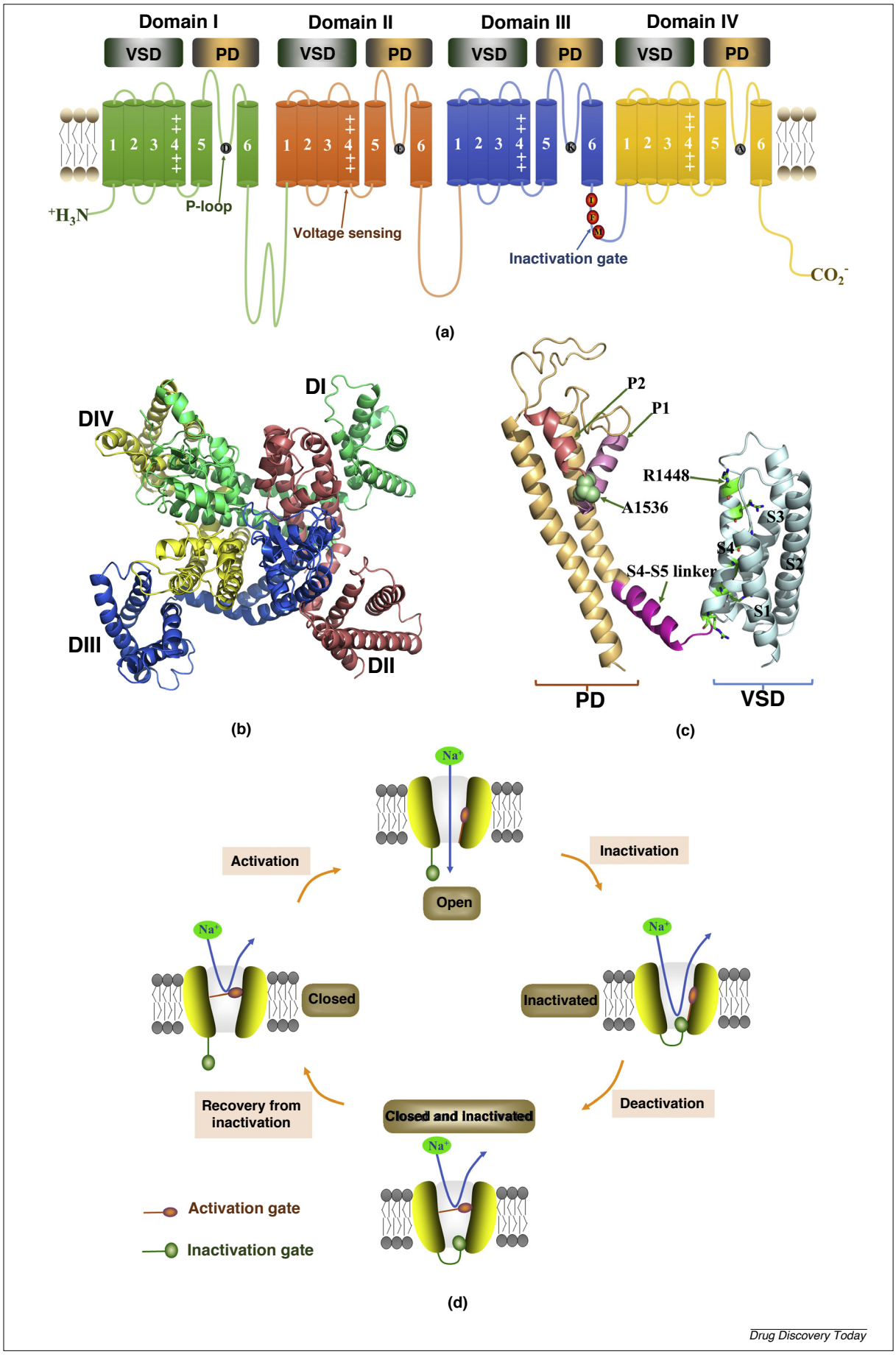
Domain I
Domain II
Domain III
Domain IV
VSD
PD
P-loop
Voltage sensing
Inactivation gate
$^{+}H_3N$
CO_2^-
(a)
DI
DII
DIII
DIV
(b)
P2
P1
R1448
A1536
S3
S4
S2
S1
S4-S5 linker
PD
VSD
(c)
Na+
Open
Activation
Inactivation
Closed
Inactivated
Recovery from inactivation
Deactivation
Closed and Inactivated
Activation gate
Inactivation gate
(d)
Drug Discovery Today

water-soluble heterocyclic guanidinium toxins (TTX and STX) and peptide μ-contoxins from the marine cone snail. Owing to the large sequence differences of site 1 in various VGSCs, guanidinium neurotoxins are valuable chemical probes to characterize the physiological functions of VGSCs. The cryo-EM structures of $hNa_v1.7$ in complex with TTX and STX determined recently suggest that their polar groups form extensive electrostatic interactions with acidic residues in the outer electronegative ring, as well as Asp and Glu in the DEKA motif, leading to the complete block of Na^+ ion entry to the SF vestibule [17].

Site 2: intracellular pore gating activator (state dependent)

Binding site 2 is generally considered to be formed by DI-S6 and DIV-S6, and can be occupied by lipid-soluble toxins with diverse chemical structures, such as batrachotoxin (BTX), veratridine (VTD), antillatoxin (ATX), aconitine (ACT), and grayanotoxin (GTX). However, BTX was considered to be localized at the inner pore with residues in the S6 of four domains [21], although it remains uncertain whether all toxins in site 2 are involved in the four S6s. These modulators contribute to activating the channel or impeding inactivation, resulting in voltage-dependence activation toward more negative potentials and channel opening at resting potentials. BTX is regarded as a full activator, whereas VTD and ACT are regarded as partial activators. These toxins preferentially bind to the open and inactivated states of VGSCs as the binding fenestration exposed [21].

Site 3: extracellular gating activator

Binding site 3 mainly locates at the extracellular S3–S4 loops of DIV, and is occupied by δ-atracotoxins from spiders, α-scorpion toxins, and anthopleurin from sea anemones. Upon binding to the closed/resting state, these toxins impair inactivation and induce a prolonged opening of VGSCs by blocking the conformational changes of DIV-S4 during fast inactivation [22].

Site 4: extracellular gating blocker

Binding site 4 mainly localizes in the extracellular loops that connect the S1–S2 and S3–S4 segments of DII. Site 4 can be recognized by long-chain peptide toxins, such as β-scorpion toxins and several spider toxins, which comprise 58–76 residues with four cross-linked disulfide bridges to stabilize the α/β structural motif. These toxins reduce the peak sodium current amplitude and shift the voltage-dependent activation toward more negative potentials by blocking the DII-VSD conformational change; however, the structural-based mechanism of action remains unclear [23].

Site 5: intracellular pore gating activator (state dependent)

Compared with binding sites 1–4, binding site 5 scattered in DI-S6 and DIV-S5 has not been well characterized and the key residues involved in this site remain elusive. This site can be occupied by highly lipophilic cyclic polyether toxins, such as ciguatoxins (CTX) and brevetoxins (PbTxs) from dinoflagellates. These toxins position themselves across the plasma membrane, parallel with the TM segments, with the A-ring facing the intracellular side and the tail terminal toward the extracellular side. These toxins preferentially bind to the activated channel and exert a multitude of electrophysiological effects by suppressing activation and shifting the activation potential toward hyperpolarized potentials [24].

Site 6: extracellular gating activator

Binding site 6 is still speculative and remains undefined. Site 6 might be occupied by δ-conotoxins, which interact with a set of conserved residues in DIV-S4, then turning out to slow down or inhibit VGSC inactivation by trapping DIV-S4 into an outward conformation without the typical voltage dependency. Although site 6 is close to site 3, their activators do not compete with each other [25].

Site 7: intracellular gating activator

Binding site 7 locates at DIII-S6 and can be occupied by some insecticides, including pyrethroids and DDT. These insecticidal agents can prolong the opening state of VGSCs by suppressing channel deactivation and inactivation, resulting in firing and depolarization of the nerve membrane in the insect nervous system [26].

Site 8: local anesthetic (LA) binding site

Binding site 8 positions in the inner cavity of the channel pore and comprises residues in S6 of DI, DIII, and DIV, which exhibits significant overlap with site 2. This site has been targeted by most VGSC drugs for the treatment of sodium channelopathies, such as local anesthetics, class I cardiac antiarrhythmics, anticonvulsants, and antidepressants, which share common structural features with a lipophilic aromatic ring and a hydrophilic tertiary amine group. However, the site is almost identical across all VGSCs. As a consequence, these drugs are nonselective VGSC blockers with state and frequency dependence [27].

Small-molecule VGSC modulators

By inhibiting the conduction of action potential through a simple pore blocking mechanism or through preferential binding to and stabilization of the channels in nonconducting inactivated states, VGSC-modulating drugs have therapeutic significance as LAs (lidocaine), general anesthetics (sevoflurane and isoflurane), anticonvulsants (carbamazepine and lamotrigine), and antiarrhythmic drugs (mexiletine) [3]. However, most of these drugs are weakly basic or neutral and bind to the highly conserved LA binding site of VGSCs; thus, they are first-generation nonselective modulators of VGSCs. The charged drugs preferentially access the binding site via the internal aqueous pathway produced by the state-dependent opening of the channels, whereas the uncharged and hydrophobic drugs with less state dependence access the binding site on closed and inactivated channels through fenestrations at the side of the pore. Given the low isoform selectivity, limited therapeutic indices, and dose-limiting adverse effects of first-generation VGSC

FIGURE 1

Overall structures and typical open–closed–inactivated cycle of voltage-gated sodium channels (VGSCs). (a) Topology of the human VGSC α-subunits. The α-subunit comprises four domains: DI (green), DII (orange), DIII (blue), and DIV (yellow). Each domain has six segments (S1–S6). Segments S1–S4 form the voltage-sensing domain (VSD). S5, S6, and the connecting P-loops form the pore domain (PD). (b) Top view of $hNa_v1.4$ [Protein Data Bank (PDB) entry: 6AGF] with partial loops removed for clarity. (c) The different segments of DIV in $hNa_v1.4$ (PDB entry: 6AGF) are shown as a cartoon. Ala1536 of the signature DEKA motif is shown as a sphere. The 'gating charge' residues on S4 are shown as sticks, with only Arg1488 labeled for clarity. (d) Please see the main text for explanation.

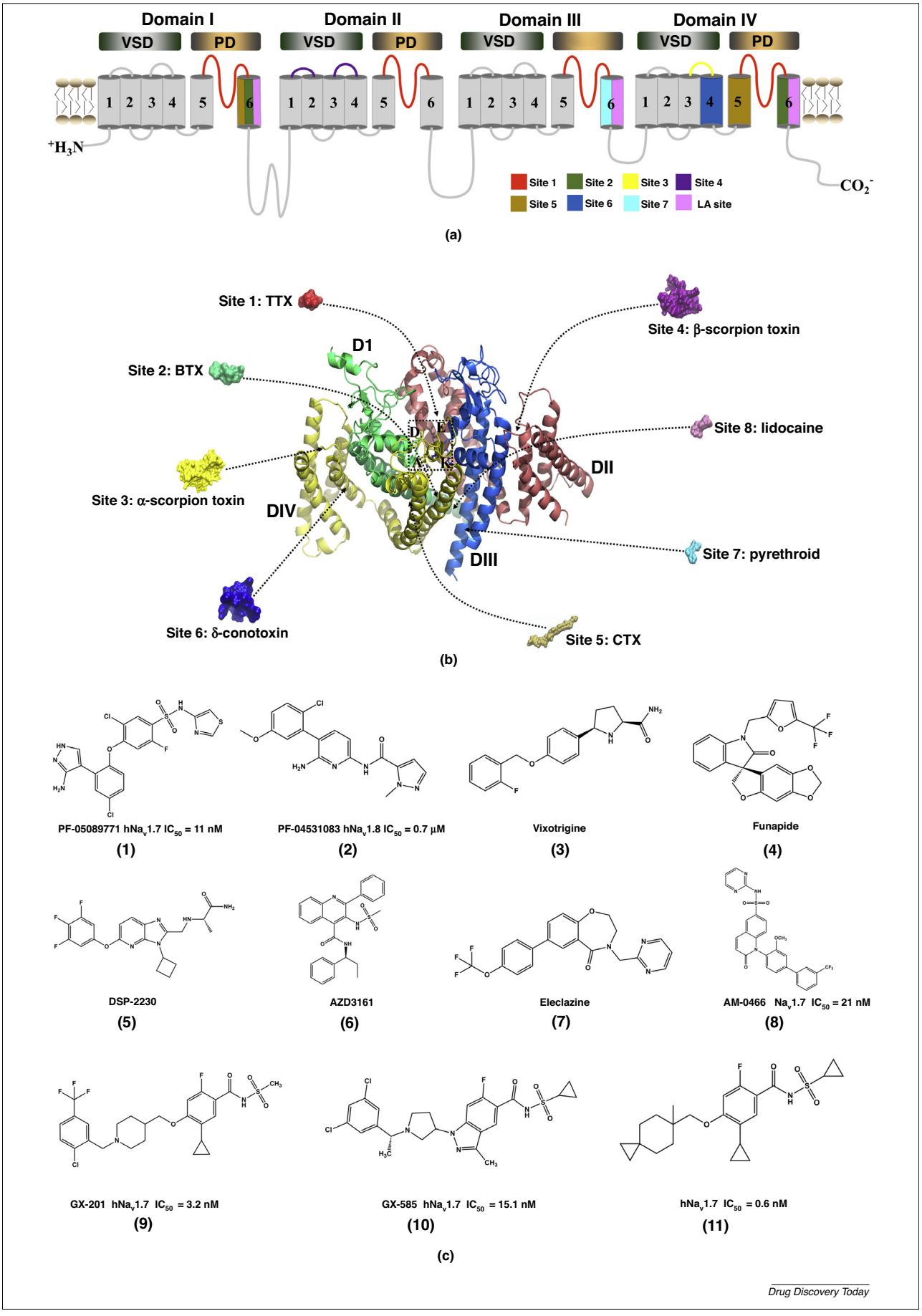
Domain I
Domain II
Domain III
Domain IV
VSD
PD
1 2 3 4 5 6
+H3N
CO2-
Site 1
Site 2
Site 3
Site 4
Site 5
Site 6
Site 7
LA site
(a)
Site 1: TTX
Site 2: BTX
Site 3: α-scorpion toxin
Site 4: β-scorpion toxin
Site 8: lidocaine
Site 7: pyrethroid
Site 5: CTX
Site 6: δ-conotoxin
D1
DII
DIII
DIV
(b)
PF-05089771 hNav1.7 IC50 = 11 nM
(1)
PF-04531083 hNav1.8 IC50 = 0.7 μM
(2)
Vixotrigine
(3)
Funapide
(4)
DSP-2230
(5)
AZD3161
(6)
Eleclazine
(7)
AM-0466 Nav1.7 IC50 = 21 nM
(8)
GX-201 hNav1.7 IC50 = 3.2 nM
(9)
GX-585 hNav1.7 IC50 = 15.1 nM
(10)
hNav1.7 IC50 = 0.6 nM
(11)
(c)
Drug Discovery Today

TABLE 1

Overview of the major VGSC binding sites

Site	Modulator	Binding domain	Pharmacological effect
1	TTX, saxitoxin (STX), μ-conotoxin	DI-IV P-loops	Pore blocker blocking Na^+ conduction
2	BTX, VTD, ACT, GTX	DI-S6, DIV-S6	Negative shift in voltage dependence of activation, persistent activation, slow and/or prevent inactivation
3	α-scorpion toxins (OD1, LqhIT), sea anemone toxins (ATX-II, AFTII)	Extracellular loops of DIV S3–S4	Destabilization of inactivation, block fast inactivation
4	β-Scorpion toxins (CssIV, Lqh-1), spider toxins (huwentoxin-IV, Hm-3, μ-agatoxin), δ-palutoxins	Extracellular loops of DII S1–S2 and DII S3–S4	Shift voltage-dependence of activation in hyperpolarizing direction, reduce amplitude of peak Na^+ currents
5	PbTx, CTX	DI-S6, DIV-S5	Enhance activation and block of inactivation, shift inactivation to more negative potentials
6	δ-conotoxin (d-SVIE, TxVIA, GmVIA)	DIV-S4	Slowing down of inactivation
7	Pyrethroids	DIII-S6	Persistent activation
8	Small-molecule drugs, local anesthetics	DI-S6, DIII-S6, DIV-S6	Hyperpolarizing shifts in steady-state inactivation, state-dependent nonselective Na^+ conduction blockers

drugs, extensive efforts have been dedicated to search for more isoform-selective and disease-specific VGSC modulators [28]. Considering that the marketed first-generation VGSC drugs have been extensively summarized [2,5], here we only focus on second-generation small molecules with superior VGSC isoform-selectivity profiles (Fig. 2c and Table 2).

Pfizer has disclosed a series of acidic diaryl ether heterocyclic sulfonamides as $Na_v1.7$-selective inhibitors. Among them, PF-04856264 inhibits $Na_v1.7$ with an IC_{50} of 28 nM and binds preferentially to the voltage-sensing region of DIV in the inactivated state. The subsequent optimization of the central phenyl ring of PF-04856264 identified the first clinical candidate, PF-05089771 (**1**, Fig. 2c) [29]. Although PF-05089771 has good oral bioavailability and pharmacokinetic profiles, it shows poor blood–brain barrier (BBB) permeability, which could limit its analgesic efficacy. Mutagenesis studies demonstrated that these compounds bind to the residues in S2 (Y1537 and W1538) and S3 (D1586) in the voltage-sensing domain IV, which has also been validated by the crystal structure of the $hNa_v1.7$ voltage-sensing domain IV in complex with an aryl sulfonamide via the 'voltage sensor trapping' mechanism [11]. A variety of isoform-selective $Na_v1.7$ inhibitors have been discovered to target the unique site and exhibit superior isoform selectivity over traditional nonselective pore region-binding ligands.

Pfizer also identified several novel $Na_v1.7$-selective inhibitors with different chemical structures [1]. In addition, PF-04531083 (**2**, Fig. 2c) has been pushed into Phase II clinical trials as a $Na_v1.8$-selective inhibitor for the treatment of postsurgical dental pain [30]. Convergence company discovered vixotrigine (**3**, Fig. 2c), a potent and selective $Na_v1.7$ inhibitor, formerly known as CNV-1014802 [31]. With good BBB permeability. vixotrigine is a selective state-dependent $Na_v1.7$ inhibitor used initially to treat chronic pain and is now in Phase III clinical trials for the treatment of trigeminal neuralgia and in Phase II clinical trials for the treatment of erythromelalgia and neuropathic pain. Convergence has also developed CNV-3000223 and CNV-3000164 as $Na_v1.7$-selective inhibitors, as well as CNV-106436 as a $Na_v1.3$-selective state-dependent inhibitor for the treatment of epilepsy and bipolar disorders, although the structures of all these inhibitors have not yet been released [1].

Xenon and Teva identified funapide (**4**, Fig. 2c), formerly known as TV-45070 or XEN402 [32], which is a selective $Na_v1.7$ and $Na_v1.8$ dual blocker for the treatment of a variety of chronic pain conditions. In 2013, funapide received the US Food and Drug Administration (FDA) orphan-drug designation as a pain-treatment drug candidate and was in Phase II clinical trials in 2014. Xenon developed XEN403/TV-4507, a selective $Na_v1.7$ blocker as a backup candidate to funapide, for the potential treatment of pain [33]. Xenon's collaborator Genentech, a member of the Roche Group, disclosed GDC-0276 and GDC-0310, which are both oral and $Na_v1.7$-selective inhibitors for the treatment of pain [34]. These molecules completed Phase I clinical trials in 2017. In addition, several inhibitors have been advanced to clinical trials, such as DSP-2230 (**5**, Fig. 2c), a $Na_v1.7$ and $Na_v1.8$ dual modulator, from Sumitomo Dainippon Pharma [35], GSK-2339345 with broad-spectrum VGSC inhibition from GlaxoSmithKline [36], AZD-3161 (**6**, Fig. 2c) with $Na_v1.7$ inhibition from AstraZeneca, Eleclazine (GS-6615) (**7**, Fig. 2c) with $Na_v1.5$ inhibition from Gilead, and NKTR-171 with broad-spectrum VGSC inhibition from Nektar [1,33].

In 2017, Graceffa *et al*. discovered a series of atropisomeric quinolinone sulfonamide $Na_v1.7$-selective inhibitors. After optimization of metabolic and pharmacokinetic properties, AM-0466 (**8**, Fig. 2c) was identified, and shows a favorable pharmacokinetic profile and robust reduction in terms of both

FIGURE 2

Major ligand-binding sites and representative isoform-selective inhibitors of voltage-gated sodium channels (VGSCs). (a) Topology of the human VGSC α-subunit binding sites. (b) View of $hNa_v1.4$ with partial loops, with S1–S4 segments of DI and DIII removed for clarity [Protein Data Bank (PDB) entry: 6AGF]. Representative peptide toxins and small-molecule modulators are labeled with arrows pointing to the major ligand-binding sites in $hNa_v1.4$. The SF region is shown by a dashed box (DEKA). Site 1 (red) comprises the four P-loops. Site 2 (green) comprises DI-S6 and DIV-S6. Site 3 (yellow) is formed by the extracellular loop connecting S3–S4 of DIV. Site 4 (purple) comprises extracellular loops connecting S1–S2 and S3–S4 of DII. Site 5 (gold) contains DI-S6 and DIV-S5. Site 6 (blue) includes DIV-S4. Site 7 (cyan) covers DIII-S6. Site 8 (pink) is the local anesthetic (LA) site located in S6 of DI-S6, DIII-S6, and DIV-S6. (c) Chemical structures of VGSC modulators undergoing clinical trials and representative isoform-selective inhibitors.

TABLE 2

Novel Na_v channels modulators undergoing clinical trials

Compound	Company	Pharmacology	Phase	Indications	Refs
PF-05089771	Pfizer	$Na_v1.7$	II	Neuropathic/Inflammatory pain erythromelalgia (oral)	[40]
PF-04531083	Pfizer	$Na_v1.8$	II	Neuropathic/Inflammatory pain (oral)	[41]
Vixotrigine	Convergence	$Na_v1.7$	III	Neuropathic pain	[42]
Funapide	Xenon/Teva	$Na_v1.7$	II	Neuropathic/Inflammatory pain erythromelalgia (topical)	[43]
XEN403	Xenon	$Na_v1.7$	I	Neuropathic/Inflammatory pain erythromelalgia (oral)	[44]
GDC0276	Xenon/Genentech	$Na_v1.7$	I	Pain	[45]
GDC-0310	Xenon/Genentech	$Na_v1.7$	I	Pain	[45]
DSP-2230	Dainippon Sumitomo	$Na_v1.7/Na_v1.8$	II	Neuropathic pain (oral)	[46]
AZD3161	AstraZeneca	$Na_v1.7$	I	Neuropathic/Inflammatory pain (IV, intradermal)	[44]
GSK-2339345	GlaxoSmithKline	Broad VGSCs	II	Cough	[47]
Eleclazine	Gilead	$Na_v1.5$	III	long QT syndrome	[44]
NKTR-171	Nektar	Broad VGSCs	I	Peripheral neuropathic pain (oral)	[44]

scratching bouts in a histamine-induced pruritus model and licking time in a capsaicin-induced nociception model of pain [37]. In 2018, Bankar *et al.* identified two second-generation $Na_v1.7$-selective inhibitors (GX-201 and GX-585) with the acylsulfonamide scaffold (Fig. 2c), which have robust analgesic activity in inflammatory and neuropathic pain models. In addition, GX-201 and GX-585 showed a relatively long half-life in mice and were suitable for once-daily dosing, and the repeat dosing of GX-585 also produced a tenfold decrease in EC_{50} for analgesia [38]. In 2018, Sun *et al.* reported a series of orally bioavailable acylsulfonamides with stronger $Na_v1.7$ inhibition over $Na_v1.5$, high efficiency in vivo models of pain and $hNa_v1.7$ target engagement. After optimization of inhibitory potency and improvement of human metabolic stability, compound **11** (Fig. 2c) was identified as the most potent (IC_{50} = 0.6 nM) and efficacious $hNa_v1.7$-selective inhibitor reported to date [39].

Molecular modeling studies of VGSCs

As complementary tools to experimental techniques, computational approaches provide a powerful way to elucidate the energetic determinants between VGSCs and various modulators, and even to characterize the dynamic processes of ion permeation, voltage gating, and ligand binding [40,41]. Representative molecular modeling studies are summarized here.

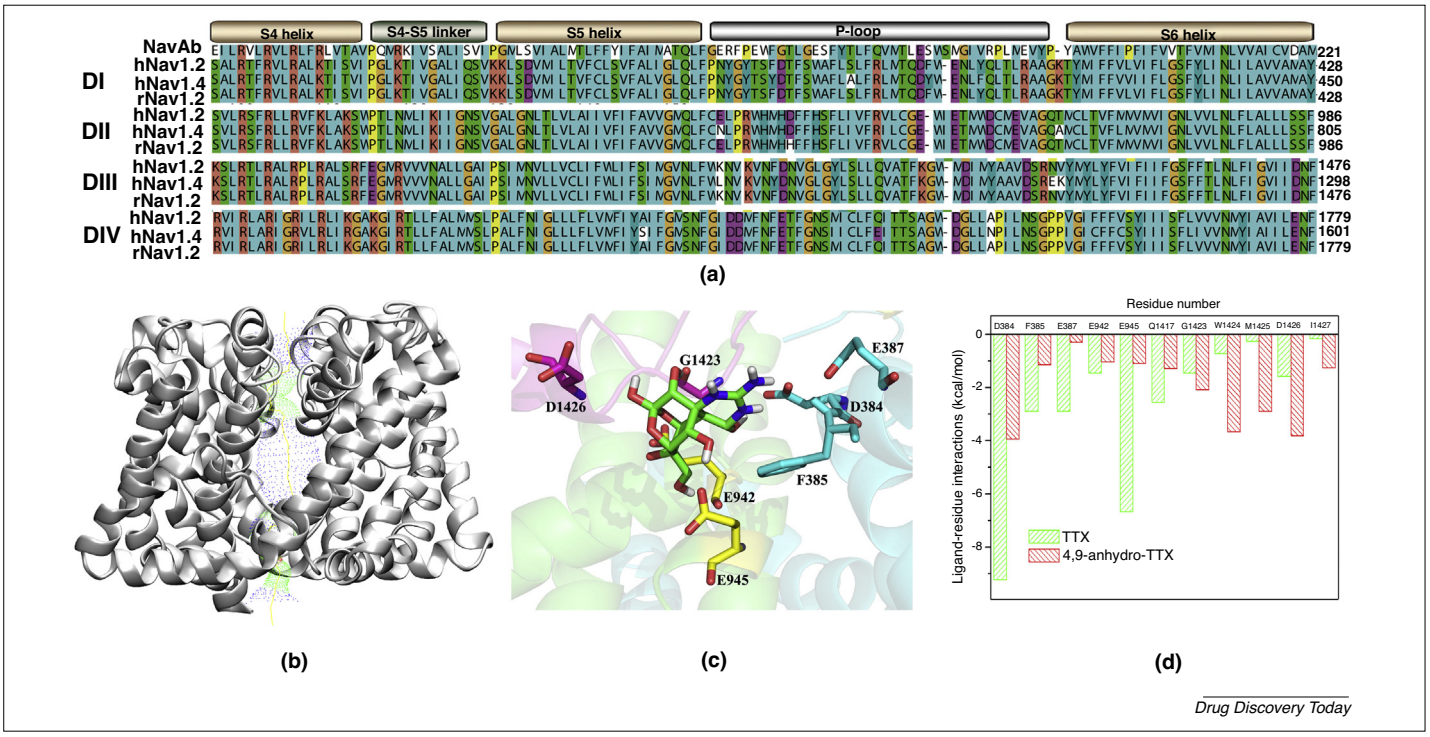

FIGURE 3

Outline of integrated computational approaches used to explore the binding mode of $hNa_v1.2$ with tetrodotoxin (TTX) analogs. (a) Sequence alignment of Na_vAb with $hNa_v1.2$, $hNa_v1.4$, and $rNa_v1.2$. (b) The permeation path of the constructed hNav1.2 model is shown by dots. (c) The binding mode of the docked modulator TTX to the key residues in $hNa_v1.2$. Carbon atoms of TTX in the docked conformation are colored in green. (d) Energy contributions of the key residues in $hNa_v1.2$.

Based on the first X-ray crystal structure of the KcsA cation channel [42], Lipkind and Fozzard constructed the central pore of $Na_v1.4$, including S5, S6, and the P-loops from each domain [43]. The outer vestibule accommodates TTX and STX, and their guanidinium groups locate toward the central axis. In 2012, Tikhonov and Zhorov constructed a Na_vAb-based homology model of $Na_v1.4$ with an adjusted sequence alignment [44], and docked TTX into the outer pore to investigate the structural properties of $Na_v1.4$ and explain the available experimental data. In 2013, Ulmschneider *et al.* carried out microsecond MD simulations to explore the ion translocation pathway and conductance process based on the crystal structure of the open conformation of a bacterial VGSC pore (Na_vMs) [9]. The predicted ion conductance and selectivity were in accordance with the electrophysiology measurements of the Na_vMs channel expressed in HEK 293 cells [45]. In 2014, Chen *et al.* built a structural model of $Na_v1.4$ based on the crystal structure of Na_vAb and investigated the model of μ-conotoxins PIIIA binding to VGSCs [46]. Six possible binding modes of $Na_v1.4$-PIIIA were submitted to the MD simulations with distance restraints, and the PMF profile for the dissociation of PIIIA from $Na_v1.4$ along the channel axis was explored by umbrella sampling simulations. In 2018, Buyan *et al.* carried out replica exchange solute tempering (REST)-biased simulations to investigate the binding mechanisms of nine compounds with Na_vMs [10] and Na_vPas [12,47]. Two distinct binding sites inside the pore were occupied by the neutral and charged drugs, respectively. The neutral compounds were located lower in the central cavity, whereas the charged structures bound more tightly and occluded the pore by extending into the base of the selectivity filter.

Recently, an integrated computational protocol was used to investigate the binding mechanisms of $hNa_v1.2$ with TTX and its metabolite 4,9-anhydro-TTX [48] (Fig. 3). The central pore of $hNa_v1.2$ was constructed based on the Na_vAb, and sequence alignment of the P-loops was generated by using the method proposed by Tikhonov and Zhorov [44] (Fig. 3a). According to a previous study [46] and experiment data [49], the structure of $hNa_v1.2$ in complex with TTX was constructed by the induced-fit docking (Fig. 3c). The computational results revealed some important contacts, including H-bond interactions between the hydroxy groups of TTX and the outer ring carboxylates of the selectivity filter, as well as a cation–π interaction between the primary amine of guanidinium and Phe385. In addition, the effect on toxin sensitivity of D384 N and E945 K mutants was explored [50]. In general, these computational results provide a valuable model to design potent and selective neurotoxins of $Na_v1.2$ and facilitate insights into the blocking mechanism of TTX to VGSCs.

Owing to the lack of the co-crystallized structure and the complexity of heteromeric TM proteins with a wealth of cavities in terms of shape, hydrophobicity, and electrostatic properties, there are rare opportunities to obtain potential VGSC modulators via virtual screening based on the homology models of VGSCs. In 2013, according to two isoform-selective VGSCs modulators with the structure of the marine alkaloid clathrodin, Tomaić *et al.* discovered several $Na_v1.7$ modulators with novel scaffolds (IC_{50} <10 μM). First, through a ROCS similarity search in the ZINC database, five state-dependent $Na_v1.3$ and $Na_v1.7$ modulators were discovered [51]. In addition, the structural model of $hNa_v1.4$ with an open-pore conformation was constructed based on the nonselective cation channel NaK and Na_vAb. TTX and the LA etidocaine were docked into the $hNa_v1.4$ model to reproduce the experimental binding data. After that, the similarity searching was followed by docking 10 000 compounds into the $hNa_v1.4$ open-pore model, whereas no compounds exhibited better activity compared with the starting modulators. The reason for the low hit rate of this screening method might be the inaccuracy of the $hNa_v1.4$ open-pore homology model based on VGKCs, which suggests a different mechanism, as revealed by the recently determined crystal structure of the open-pore bacterial sodium channel (Na_vMs) [9].

Concluding remarks and future perspectives

VGSCs have received extensive interest from the academic and pharmaceutical communities alike. However, currently available VGSC drugs are nonselective for the VGSC family, resulting in adverse effects and often limited therapeutic indices as a result of the lack of an exact understanding of their molecular targets and mechanisms of action. Therefore, developing potent and isoform-selective VGSC modulators with favorable pharmacokinetic profiles is crucial for the treatment of VGSC-associated diseases. Owing to a wealth of genetic evidence associated with the pain-processing pathway, $Na_v1.7$ has been the focus of intense investigation in recent years. One of the primary challenges to design $Na_v1.7$ inhibitors is the isoform selectivity over other VGSCs; acceptable selectivity over $Na_v1.5$ is particularly important, because it is responsible for cardiovascular function. Recently, a class of arylsulfonamide and acylsulfonamide $Na_v1.7$-selective inhibitors were reported, which can be used as promising starting points for further optimization, although most of them are zwitterionic (a basic nitrogen) and bind to the positively charged R4 on S4 of VSD IV, resulting in poor permeability and low oral bioavailability. To date, three extracellular druggable sites of $Na_v1.7$, including the extracellular vestibule of the pore, the extracellular loops of VSD II and the extracellular loops of VSD IV, exhibit the highest potential for the discovery of $Na_v1.7$-selective inhibitors.

VGSCs are sophisticated membrane proteins that can rapidly transit across different states, and thus it is difficult to assess the state dependence of ligand binding. Although most marketed VGSC drugs exert their effect by stabilizing the inactivated state, it remains to be determined whether state dependence is a desirable feature for a selective $Na_v1.7$ modulator. In addition, the sequence differences and functional specialization of the four VSDs in eukaryotic VGSCs make VSDs viable targets for designing isoform-selective modulators based on the structural determinants of the toxin–channel interaction. Genetic mutations in the β subunits are associated with a variety of diseases, and thus β-subunits could be novel therapeutic targets for future drug discovery. Further studies are needed to clarify the biology of these crucial proteins and their potentials as novel therapeutic targets. In recent years, a serial of high-resolution structures of VGSCs have been determined, and high-throughput automated patch clamp (APC) assays have been developed to detect state-dependent channel modulators. In general, such progress has contributed to providing new

insights into structure–function relationships and the discovery of novel VGSC drugs.

Acknowledgments

This study was supported by the National Science & Technology Major Project of China ''Key New Drug Creation and Manufacturing Program" (2018ZX09711002-007), the National Key R&D Program of China (2016YFB0201700), the National Science Foundation of China (21575128, 81773632 and 81803430), the Natural Science Foundation of Jiangsu Province (No. BK20150247), Six Talent Peaks Project in Jiangsu Province (No. 2017-XNY-015), and Qing Lan Project.

References

1 de Lera Ruiz, M. and Kraus, R.L. (2015) Voltage-gated sodium channels: structure, function, pharmacology, and clinical indications. *J. Med. Chem.* 58, 7093–7118
2 Bagal, S.K. *et al.* (2015) Voltage gated sodium channels as drug discovery targets. *Channels* 9, 360–366
3 Carnevale, V. and Klein, M.L. (2017) Small molecule modulation of voltage gated sodium channels. *Curr. Opin. Struct. Biol.* 43, 156–162
4 Huang, W. *et al.* (2017) Structure-based assessment of disease-related mutations in human voltage-gated sodium channels. *Protein Cell* 8, 401–438
5 Nardi, A. *et al.* (2012) Advances in targeting voltage-gated sodium channels with small molecules. *ChemMedChem* 7, 1712–1740
6 Payandeh, J. *et al.* (2011) The crystal structure of a voltage-gated sodium channel. *Nature* 475, 353–358
7 Zhang, X. *et al.* (2012) Crystal structure of an orthologue of the NaChBac voltage-gated sodium channel. *Nature* 486, 130–134
8 Payandeh, J. *et al.* (2012) Crystal structure of a voltage-gated sodium channel in two potentially inactivated states. *Nature* 486, 135–139
9 McCusker, E.C. *et al.* (2012) Structure of a bacterial voltage-gated sodium channel pore reveals mechanisms of opening and closing. *Nat. Commun.* 3, 1102
10 Bagnéris, C. *et al.* (2014) Prokaryotic NavMs channel as a structural and functional model for eukaryotic sodium channel antagonism. *Proc. Natl. Acad. Sci. U. S. A.* 111, 8428–8433
11 Ahuja, S. *et al.* (2015) Structural basis of Nav1.7 inhibition by an isoform-selective small-molecule antagonist. *Science* 350 aac5464
12 Shen, H. *et al.* (2017) Structure of a eukaryotic voltage-gated sodium channel at near–atomic resolution. *Science* 355 eaal4326
13 Yan, Z. *et al.* (2017) Structure of the Nav1.4-β1 complex from electric eel. *Cell* 170, 470–482
14 Pan, X. *et al.* (2018) Structure of the human voltage-gated sodium channel Nav1.4 in complex with β1. *Science* 362 eaau2486
15 Shen, H. *et al.* (2018) Structural basis for the modulation of voltage-gated sodium channels by animal toxins. *Science* 362 eaau2596
16 Pan, X. *et al.* (2019) Molecular basis for pore blockade of human Na+ channel Nav1.2 by the μ-conotoxin KIIIA. *Science* 363, 1309–1313
17 Shen, H. *et al.* (2019) Structures of human Nav1.7 channel in complex with auxiliary subunits and animal toxins. *Science* 363, 1303–1308
18 Bagal, S.K. *et al.* (2012) Ion channels as therapeutic targets: a drug discovery perspective. *J. Med. Chem.* 56, 593–624
19 Yang, N. *et al.* (1996) Molecular basis of charge movement in voltage-gated sodium channels. *Neuron* 16, 113–122
20 Zhang, F. *et al.* (2013) Shellfish toxins targeting voltage-gated sodium channels. *Mar. Drugs* 11, 4698–4723
21 Du, Y. *et al.* (2011) Identification of new batrachotoxin-sensing residues in segment IIIS6 of sodium channel. *J. Biol. Chem.* 286, 13151–13160
22 Hampl, M. *et al.* (2016) Sodium channel slow inactivation interferes with open channel block. *Sci. Rep.* 6, 25974
23 Stevens, M. *et al.* (2011) Neurotoxins and their binding areas on voltage-gated sodium channels. *Front Pharmacol.* 2, 71
24 Turner, A. *et al.* (2015) Potential threats posed by new or emerging marine biotoxins in UK waters and examination of detection methodology used in their control: brevetoxins. *Mar. Drugs.* 13, 1224–1254
25 Leipold, E. *et al.* (2005) Molecular interaction of δ-conotoxins with voltage-gated sodium channels. *FEBS Lett.* 579, 3881–3884
26 Soderlund, D.M. (2010) State-dependent modification of voltage-gated sodium channels by pyrethroids. *Pestic. Biochem. Physiol.* 97, 78–86
27 England, S. and De Groot, M.J. (2009) Subtype-selective targeting of voltage-gated sodium channels. *Br. J. Pharmacol.* 158, 1413–1425
28 Weiss, M.M. *et al.* (2017) Sulfonamides as selective Nav1.7 inhibitors: optimizing potency and pharmacokinetics while mitigating metabolic liabilities. *J. Med. Chem.* 60, 5969–5989
29 Theile, J.W. *et al.* (2016) The selective Nav1.7 inhibitor, PF-05089771, interacts equivalently with fast and slow inactivated Nav1.7 channels. *Mol. Pharmacol.* 95, 540–548
30 Bagal, S.K. *et al.* (2015) Discovery and optimization of selective Nav1.8 modulator series that demonstrate efficacy in preclinical models of pain. *ACS Med. Chem. Lett.* 6, 650–654
31 Deuis, J.R. *et al.* (2016) Analgesic effects of GpTx-1, PF-04856264 and CNV1014802 in a mouse model of NaV1.7-mediated pain. *Toxins* 8, 78
32 Sclafani, J.A. *et al.* (2017) The first asymmetric pilot-scale synthesis of TV-45070. *Org. Process Res. Dev.* 21, 1616–1624
33 Bagal, S.K. *et al.* (2014) Recent progress in sodium channel modulators for pain. *Bioorg. Med. Chem. Lett.* 24, 3690–3699
34 Emery, E.C. *et al.* (2016) Nav1.7 and other voltage-gated sodium channels as drug targets for pain relief. *Expert Opin. Ther. Tar.* 20, 975–983
35 Martz, L. (2014) Nav-i-gating antibodies for pain. *Science-Business eXchange* 7 662–662
36 Smith, J.A. *et al.* (2017) Effects of a novel sodium channel blocker, GSK2339345, in patients with refractory chronic cough. *Int. J. Clin. Pharmacol. Ther.* 55, 712–719
37 Graceffa, R.F. *et al.* (2017) Sulfonamides as selective NaV1.7 inhibitors: optimizing potency, pharmacokinetics, and metabolic properties to obtain atropisomeric quinolinone (AM-0466) that affords robust *in vivo* activity. *J. Med. Chem.* 60, 5990–6017
38 Bankar, G. *et al.* (2018) Selective NaV1.7 antagonists with long residence time show improved efficacy against inflammatory and neuropathic pain. *Cell Rep.* 24, 3133–3145
39 Sun, S. *et al.* (2019) Identification of selective acyl sulfonamide-cycloalkylether inhibitors of the voltage gated sodium channel (NaV) 1.7 with potent analgesic activity. *J. Med. Chem.* 62, 908–927
40 Zhorov, B. and Tikhonov, D. (2016) Computational structural pharmacology and toxicology of voltage-gated sodium channels. *Curr. Top. Membr.* 78, 117–144
41 Chen, R. *et al.* (2017) Voltage-gated sodium channel pharmacology: insights from molecular dynamics simulations. *Adv Pharmacol.* 79, 255–285
42 Doyle, D.A. *et al.* (1998) The structure of the potassium channel: molecular basis of K + conduction and selectivity. *Science* 280, 69–77
43 Lipkind, G.M. and Fozzard, H.A. (2000) KcsA crystal structure as framework for a molecular model of the Na+ channel pore. *Biochemistry* 39, 8161–8170
44 Tikhonov, D.B. and Zhorov, B.S. (2012) Architecture and the pore block of eukaryotic voltage-gated sodium channels in view of the NavAb bacterial sodium channel structure. *Mol. Pharmacol.* 82, 97–104
45 Ulmschneider, M.B. *et al.* (2013) Molecular dynamics of ion transport through the open conformation of a bacterial voltage–gated sodium channel. *Proc. Natl. Acad. Sci. U. S. A.* 110, 6364–6369
46 Chen, R. and Chung, S.H. (2014) Mechanism of tetrodotoxin block and resistance in sodium channels. *Biochem. Biophys. Res. Commun.* 446, 370–374
47 Buyan, A. *et al.* (2018) Protonation state of inhibitors determines interaction sites within voltage-gated sodium channels. *Proc. Natl. Acad. Sci. U. S. A.* 115, E3135–E3144
48 Xu, L. *et al.* (2018) Insight into tetrodotoxin blockade and resistance mechanisms of Nav1.2 sodium channel by theoretical approaches. *Chem. Biol. Drug. Desi.* 92, 1445–1457
49 Terlau, H. *et al.* (1991) Mapping the site of block by tetrodotoxin and saxitoxin of sodium channel-Ii. *FEBS Lett.* 293, 93–96
50 Pusch, M.N. *et al.* (1991) Single point mutations of the sodium channel drastically reduce the pore permeability without preventing its gating. *Eur. Biophys. J.* 20, 127–133
51 Tomašić, T. *et al.* (2013) Ligand-and structure-based virtual screening for clathrodin-derived human voltage-gated sodium channel modulators. *J. Chem. Inf. Model.* 53, 3223–3232